

Incoherent shock waves in long-range optical turbulence



G. Xu^a, J. Garnier^b, D. Faccio^c, S. Trillo^d, A. Picozzi^{a,*}

^a Laboratoire Interdisciplinaire Carnot de Bourgogne (ICB), UMR 6303 CNRS - Université Bourgogne Franche-Comté, F-21078 Dijon, France

^b Laboratoire de Probabilités et Modèles Aléatoires, University Paris Diderot, 75205 Paris Cedex 13, France

^c School of Engineering and Physical Sciences, SUPA, Heriot-Watt University, Edinburgh EH14 4AS, UK

^d Department of Engineering, University of Ferrara, Via Saragat 1, 44122 Ferrara, Italy

ARTICLE INFO

Article history:

Received 1 September 2015

Accepted 28 February 2016

Available online 4 March 2016

Keywords:

Dispersive shock waves

Optical turbulence

Random nonlinear waves

ABSTRACT

Considering the nonlinear Schrödinger (NLS) equation as a representative model, we report a unified presentation of different forms of incoherent shock waves that emerge in the long-range interaction regime of a turbulent optical wave system. These incoherent singularities can develop either in the temporal domain through a highly noninstantaneous nonlinear response, or in the spatial domain through a highly nonlocal nonlinearity. In the temporal domain, genuine dispersive shock waves (DSW) develop in the spectral dynamics of the random waves, despite the fact that the causality condition inherent to the response function breaks the Hamiltonian structure of the NLS equation. Such spectral incoherent DSWs are described in detail by a family of singular integro-differential kinetic equations, e.g. Benjamin–Ono equation, which are derived from a nonequilibrium kinetic formulation based on the weak Langmuir turbulence equation. In the spatial domain, the system is shown to exhibit a large scale global collective behavior, so that it is the fluctuating field as a whole that develops a singularity, which is inherently an incoherent object made of random waves. Despite the Hamiltonian structure of the NLS equation, the regularization of such a collective incoherent shock does not require the formation of a DSW – the regularization is shown to occur by means of a different process of coherence degradation at the shock point. We show that the collective incoherent shock is responsible for an original mechanism of spontaneous nucleation of a phase-space hole in the spectrogram dynamics. The robustness of such a phase-space hole is interpreted in the light of incoherent dark soliton states, whose different exact solutions are derived in the framework of the long-range Vlasov formalism.

© 2016 Elsevier B.V. All rights reserved.

1. Introduction

Shock waves have been thoroughly investigated during the last century in many different branches of physics [1]. The well-known phenomenon of viscous shock wave in a dissipative compressible fluid (gas) is characterized by a steep jump in gas velocity, density, and temperature across which dissipation of energy due to particle collisions regularizes the shock singularity. On the other hand, in conservative systems a different regularization occurs that entails the formation, owing to dispersion, of rapidly oscillating non-stationary structures, so-called undular bores or dispersive shock waves (DSWs). Their theoretical study was pioneered in plasma physics [2,3] and water waves [4], and was readily followed by lab observations [5,6]. Seminal contributions arose afterward in

the context of the celebrated integrable Korteweg–De Vries (KdV) equation, both in terms of construction of non-stationary DSWs [7] based on Whitham modulation theory [8] and a formulation of the weak dispersion limit based on inverse scattering [9]. However, it became soon clear that DSW phenomena constitute a universal signature of singular nonlinear wave behavior in Hamiltonian models, regardless of the property of integrability [10,11]. Such behavior has generated continued interest among diverse areas of physics, ranging from the interpretation of natural phenomena such as atmospheric gravity waves [12], oceanic internal waves [13], or tidal bores [14], to lab experiments in Bose–Einstein condensates [15], unitary Fermi gases [16], nonlinear optics (temporal [17], and spatial [18] phenomena, as well as a diversity of optical settings [19]), quantum liquids [20], nonlinear chains or granular materials [21], viscous fluids [22], and electron beams [23]. Also notice that the role of *structural disorder of the medium* on the properties of DSWs has been investigated in the context of optical waves [24,25].

These previous studies on DSWs have been essentially reported for coherent, i.e., deterministic, wave envelopes. When studying,

* Corresponding author. Tel.: +33 380395979; fax: +33 380395971.

E-mail address: Antonio.Picozzi@u-bourgogne.fr (A. Picozzi).

vice versa, a system of fully random nonlinear waves (a speckle beam in the language of optics), the usual dynamics of DSW formation is challenged, yet the formation of incoherent shocks becomes possible through different mechanisms, as we have shown in two recent works [26,27]. In this respect, it is important to remind that an accurate statistical description of a system of random waves has been developed in the weakly nonlinear regime by the so-called wave turbulence theory, which has been successfully applied to a huge variety of physical systems [28–35]. However, such an approach is known to break down for strong nonlinearities, when the turbulent system can be heavily affected by nonlinear excitations, such as shock waves, vortices, (quasi-)solitons, collapsing wavepackets, or rogue waves [30–32,35–42]. In this general framework, we recently explored how shock wave singular behaviors can spontaneously emerge within two particular types of turbulent systems which are frequently encountered in the context of optical waves.

(i) On the one hand, we considered the temporal dynamics of a random wave that propagates in a defocusing nonlinear medium characterized by a temporal noninstantaneous nonlinear response (i.e., temporal nonlocality). In this case, at variance with the deterministic case where breaking occurs in time domain [17], the field retains a random structure in time, while exhibiting a wave breaking process (“gradient catastrophe”) in frequency which leads to incoherent DSWs in the Fourier spectral dynamics [26,43]. On the basis of a weakly nonlinear wave turbulence approach, the spectral dynamics of the incoherent wave can be described in the framework of a nonequilibrium kinetic equation whose structure is formally analogous to that considered to study weak Langmuir turbulence (WLT) in plasmas [34,35]. Note that this formalism proved efficient in describing different optical phenomena [35], such as the formation of spectral incoherent solitons [44,45] through supercontinuum generation [46]. In Ref. [26] we showed that spectral incoherent DSWs can be described in detail by a family of singular integro-differential kinetic equations (SID-KE), which were derived from the WLT kinetic equation in the limit of a long-range nonlinear interaction, i.e., a highly noninstantaneous response of the nonlinearity. This approach revealed interesting links with the 3D vorticity equation in incompressible fluids [47], or the integrable Benjamin–Ono (BO) equation [48] originally derived in hydrodynamics for stratified fluids and recently investigated in the semi-classical limit to study coherent wave breaking processes [49].

(ii) On the other hand, we considered the (transverse) spatial dynamics of a random wave that propagates in a nonlinear medium characterized by a highly nonlocal nonlinear response, i.e., spatial long-range interaction. A wave turbulence approach of the problem revealed that this regime is described in detail by a nonequilibrium long-range Vlasov formalism [50]. Note that this kinetic formulation differs from the traditional Vlasov equation describing random waves in hydrodynamics [37,40,41], in plasmas [51], or in optics, such as e.g., incoherent modulational instabilities [35,52], or incoherent solitons [52–54], while its structure is formally analogous to that describing systems of particles with long-range, e.g., gravitational, interactions [55,56]. In a recent work [27], we reported both theoretically and experimentally, a characteristic transition in the turbulent system: By strengthening the nonlocal character of the nonlinear response, the system evolves from a fully turbulent regime featuring a sea of coherent small-scale dispersive shock-waves (‘shocklets’) toward the unexpected emergence of a giant collective incoherent shock wave. The originality of this latter phenomenon of collective shock stems from the fact that, as a result of the underlying long-range interaction, the system exhibits a global collective behavior, in the sense that it is the random wave as a whole which leads to the formation of a shock wave: The shock singularity is inherently an

incoherent object itself made of random waves. As a consequence of this collective behavior, the regularization of the incoherent shock does not require the formation of a DSW structure – the regularization occurs by means of a mechanism of coherence degradation that occurs at the shock front [27].

Considering the nonlinear Schrödinger (NLS) equation as a representative model, we provide in this article a unified presentation of these two different forms of incoherent shock singularities that develop in the long range interaction regime of the turbulent system. In Section 2 we give a brief overview on spectral incoherent DSWs, in particular by underlying the essential properties which distinguish them from the collective incoherent shock waves discussed in Section 3. In this respect, we remark that both cases challenge the usual scheme underlying the DSW formation in Hamiltonian systems, since (i) in the temporal case, genuine oscillatory DSW structures are formed (though in Fourier space), in spite of the fact that the model equation is non-Hamiltonian due to the causality constraint, whereas (ii) the usual deterministic DSW regularization is ‘inhibited’ in the spatial case, in spite of the Hamiltonian structure of the spatial NLS equation. An other remarkable difference is that the development of collective incoherent shocks requires, as usual, a strong nonlinear interaction, whereas spectral incoherent DSWs are generated in the weakly nonlinear turbulent regime. In Section 3 we provide further physical insight into the nature of the collective incoherent shock wave recently observed in Ref. [27]. At variance with [27], we consider here the dynamics of a random nonlinear wave characterized by a hole in its envelope profile. Despite the underlying Hamiltonian structure of the system, such a hole perturbation usually exhibits a damping during the evolution, so that the system irreversibly relaxes toward an unperturbed homogeneous state as a result of an effective Landau-damping effect. However, in the strong nonlinear regime, we show that the system exhibits an incoherent shock singularity for the momentum and a collapse singularity for the intensity envelope of the random wave. The numerical simulations reveal that the regularization of such a double shock-collapse singularity is responsible, after a complex transient process, for the nucleation of a peculiar spectrogram hole in phase-space. This phase-space hole collective structure proves extremely robust in the system evolution, a property which we interpret in the light of incoherent dark soliton solutions that we derive from the long-range Vlasov equation. The analysis reveals that such incoherent dark soliton states cannot be clearly identified through the usual intensity analysis in real space, while their very nature appears to be ‘hidden’ in the phase-space representation.

2. Temporal domain: Spectral incoherent DSWs

2.1. Temporal nonlocal NLS equation

In this section we provide a brief overview on the nature of spectral incoherent DSWs which develop in the spectral dynamics of a random wave that evolves in a noninstantaneous nonlinear environment. The starting point is the temporal version of the NLS equation accounting for a delayed nonlinear response:

$$i\partial_z\psi = -s\partial_{tt}\psi + \psi \int R(t-t') |\psi|^2(t') dt'. \quad (1)$$

As usual in optics, the propagation distance z plays the role of an evolution ‘time’ variable, while the time (t) plays the role of the spatial variable [57]. The response function $R(t)$ is constrained by the causality condition, $R(t) = 0$ for $t < 0$, and the typical width of $R(t)$ denotes the nonlinear response time, τ_R . The problem has been normalized with respect to the ‘healing time’ $\tau_0 =$

$\sqrt{|\beta_2|L_{nl}/2}$, where β_2 is the (second-order) dispersion coefficient [$s = \text{sign}(\beta_2)$], $L_{nl} = 1/(\gamma\rho)$ the nonlinear length, γ the nonlinear coefficient, and ρ the average wave intensity. We remind that the ‘healing time’, τ_0 , denotes the typical time scale for which linear and nonlinear effects are of the same order in the limit of an instantaneous nonlinearity, e.g., the typical size of a soliton or the modulational instability period. The dimensional variables can be recovered through the substitution $\psi \rightarrow \psi\sqrt{\rho}$, $t \rightarrow t\tau_0$, $z \rightarrow zL_{nl}$. According to this normalization, $\rho = \mathcal{N}/T = T^{-1} \int_0^T |\psi|^2 dt = 1$, where T is the temporal numerical window. To integrate numerically the NLS equation (1), we make use of periodic boundary conditions in t space.

The causality condition of $R(t)$ breaks the translational invariance and the ‘time’ (z) reversibility of the NLS equation, so that Eq. (1) is not Hamiltonian, and solely conserves the total ‘power’ of the field, $\mathcal{N} = \int |\psi|^2(t, z) dt$. In the following we consider the *weakly nonlinear regime* of interaction, in which the rapid fluctuations of the random wave make linear dispersive effects dominant with respect to nonlinear effects: $L_d \ll L_{nl}$ (or equivalently $t_c \ll \tau_0$), $L_d = 2t_c^2/|\beta_2|$ being the dispersion length and t_c the correlation time of the random field $\psi(z, t)$.

According to linear response theory, the causality condition imposes restrictions on the Fourier transform of the response function, $R(t)$, whose real and imaginary parts are related by the Kramers–Krönig relations. The imaginary part is an odd function, it is known to play the role of nonlinear spectral gain, $g(\omega) = \Im[\int_0^\infty R(t)e^{-i\omega t} dt]$, which is responsible for an energy transfer from high- to small-frequency components of the random wave [35]. The typical width of $g(\omega)$ denotes the natural spectral scale of the problem, $\Delta\omega_g \sim \tau_R^{-1}$.

2.2. Weak Langmuir turbulence kinetic equation

The dynamics of random waves ruled by the NLS equation (1) is inherently stochastic, so that physical insight into the underlying deterministic behavior of DSWs is obtained by means of a statistical averaging over the realizations. The wave turbulence theory is known to provide a statistical description of the random wave system in the weakly nonlinear regime of interaction, $L_d \ll L_{nl}$. In this regime, the fluctuations of the random wave exhibit a (quasi-)Gaussian statistics, so that one can achieve a closure of the infinite hierarchy of moment equations for the random wave system [28–31,33]. In the present case, we assume that the random wave exhibits a homogeneous statistics, so that the corresponding wave spectrum results δ -correlated, $\langle \tilde{\psi}(\omega + \Omega/2, z) \tilde{\psi}^*(\omega - \Omega/2, z) \rangle = n_\omega(z) \delta(\Omega)$, where $\tilde{\psi}(\omega, z) = \int_{-\infty}^{+\infty} \psi(t, z) \exp(-i\omega t) dt$. It can be shown that, as a consequence of the causality condition inherent to the temporal response function $R(t)$, the dynamics of the averaged spectrum is governed by the following WLT integro-differential kinetic equation [44,35,34,58]:

$$\partial_z n_\omega(z) = \frac{1}{\pi} n_\omega(z) \int g(\omega - \omega') n_{\omega'}(z) d\omega'. \quad (2)$$

This equation conserves two important quantities, the total power, $\mathcal{N} = \frac{1}{2\pi} \int n_\omega(z) d\omega$, and the ‘nonequilibrium’ entropy, $\mathcal{S} = \frac{1}{2\pi} \int \log(n_\omega(z)) d\omega$, this latter property being consistent with the fact that Eq. (2) is reversible in ‘time’ (z). Also note that WLT equation (2) does not account for dispersion effects (parameter s), although the role of dispersion in its derivation is essential in order to verify the weakly nonlinear criterion, $L_d/L_{nl} \ll 1$. On the other hand, nonlinear dispersive effects, such as a frequency dependence of the nonlinear Kerr coefficient (γ becomes a function $\gamma(\omega)$) or self-steepening effects, have been shown to substantially modify the WLT equation (2), see Refs. [43,58].

2.3. Reduction to singular integro-differential kinetic equations

It has been shown that, if the initial spectral width of the random wave, say $\Delta\omega$, is of the same order as the width of the gain spectrum, $\Delta\omega \sim \Delta\omega_g$, then the system self-organizes into spectral incoherent solitons [35], i.e., a spectrally localized traveling wave solution of Eq. (2) that travels with a constant velocity in frequency space. Note that, because of the homogeneous statistics of the random wave, such incoherent soliton states cannot be identified in the spatio-temporal domain, but solely in frequency space [44]. On the other hand, in the regime where $\Delta\omega \gg \Delta\omega_g$, the spectral dynamics of the random wave develops singularities. In this ‘long-range regime’, the behavior of the tail of the gain spectrum $g(\omega)$ plays a key role in the spectral dynamics. In this respect, it is important to note that, because of the causality condition of $R(t)$, the function $g(\omega)$ always decays algebraically at infinity, e.g., $\sim 1/\omega^3$ for a damped harmonic oscillator response, or $\sim 1/\omega$ for an exponential response function. Such a slow decay introduces singularities into the convolution operator of WLT equation (2), $M_\omega = \int g(\omega - u) n_u(z) du$, which in turn leads to divergent integrals. Such singularities can be addressed accurately by introducing the Hilbert operator, $\mathcal{H}f(\omega) = \pi^{-1} \mathcal{P} \int_{-\infty}^{+\infty} \frac{f(\omega-u)}{u} du$, where \mathcal{P} denotes the Cauchy principal value. It was shown in the Supplemental material of Ref. [26] that the convolution operator can be written in the following form *without any approximations*:

$$M_\omega = -\frac{\pi \bar{R}(0)}{\tau_R} \mathcal{H}n_\omega + \frac{\pi \bar{R}^{(1)}(0)}{\tau_R^2} \partial_\omega n_\omega + \frac{\pi \bar{R}^{(2)}(0)}{2\tau_R^3} \mathcal{H} \partial_\omega^2 n_\omega + \frac{1}{\tau_R^4} \int_0^\infty [\partial_\omega^3 n_{\omega+\frac{u}{\tau_R}} + \partial_\omega^3 n_{\omega-\frac{u}{\tau_R}}] G^0(u) du, \quad (3)$$

where we have defined for $u > 0$: $G^0(u) = -\frac{1}{2} \int_u^\infty (g_v^0 + \frac{\bar{R}(0)}{v} - \frac{\bar{R}^{(2)}(0)}{v^3})(v-u)^2 dv$. Here, $\bar{R}(t)$ is a smooth function defined by $R(t) = \tau_R^{-1} \bar{R}(t/\tau_R) H(t)$, $\bar{R}^{(n)}(0)$ is the n th derivative at $t = 0$, $H(t)$ is the Heaviside step function and $g_v^0 = \Im(\int_0^\infty \bar{R}(s) \exp(-ivs) ds)$. The derivation of Eq. (3) was reported in detail in the Supplemental material of Ref. [26].

2.3.1. Spectral collapse singularity

Considering the ‘long-range’ regime $\tau_R \gg 1$ ($\tau_R \gg \tau_0$ in dimensional units), the expression of the convolution operator in (3) reveals that the spectral dynamics of the random wave changes in a dramatic way depending on the behavior of the response function near the origin, $t = 0$. The first term in Eq. (3) can only play a role provided that the response function is discontinuous at $t = 0$ ($\bar{R}(0) \neq 0$). This property is encountered with the familiar example of the exponential response function, $R(t) = H(t) \exp(-t/\tau_R)/\tau_R$. In this case the dominant term of the SID-KE takes the form, $\partial_z n_\omega(z) = -\frac{1}{\tau_R} n_\omega \mathcal{H}n_\omega$. This equation was considered as a 1D model of the vorticity formulation of the 3D Euler equation of incompressible fluid flows [47]. On the basis of the analytical solution of this equation [47], we showed that the spectral dynamics of the random wave exhibits a collapse singularity, while the corresponding spectral peak is shifted toward the low-frequency components with a constant velocity in frequency space. Note that such a spectral collapse singularity is regularized by the nonlinear dispersive term (i.e., third-term) in Eq. (3). This remarkable effect of spectral collapse predicted by the leading order term in (3) has been confirmed by the numerical simulations of the NLS equation (1) with stochastic initial conditions. It is also interesting to note that this spectral collapse singularity can be interpreted in analogy with a process condensation, in the sense that the spectrum of the random wave tends to concentrate near by a particular frequency. However, contrarily to the conventional NLS condensation process

that results from the natural thermalization toward the thermodynamic Rayleigh–Jeans equilibrium state [33,59], here the effect of ‘condensation’ occurs in 1D and very far from thermal equilibrium. We refer the interested reader to Ref. [26] and its Supplemental for more details on this spectral collapse singular behavior.

2.3.2. Spectral incoherent DSWs

The first term in the expansion of the convolution operator in (3) becomes irrelevant whenever the response function is continuous at $t = 0$. This occurs for instance for a damped harmonic response function, which is known to model the stimulated Raman scattering in optical fiber systems [57], $R(t) = H(t) \frac{1+\eta^2}{\eta\tau_R} \sin(\eta t/\tau_R) \exp(-t/\tau_R)$. In this case $\bar{R}^{(0)}(0) = 0$, so that plugging (3) into (2), one obtains the SID-KE:

$$\partial_z n_\omega = \frac{1+\eta^2}{\tau_R^2} \left(n_\omega \partial_\omega n_\omega - \frac{1}{\tau_R} n_\omega \mathcal{H} \partial_\omega^2 n_\omega \right). \quad (4)$$

The leading-order Burgers term in (4) leads to a self-steepening of the low-frequency front of the spectrum, whose gradient catastrophe is eventually arrested by the second nonlinear dispersive term involving the Hilbert operator. In this way, the spectral dynamics of the random wave leads to the formation of a DSW undular structure, see Fig. 1 in Ref. [26]. Note however that the rapid oscillatory spectral wave train induced by the shock cannot be interpreted in this case as a genuine ‘soliton train’. Indeed, contrary to the dynamics ruled by integrable models where the solitons quickly stabilize as they emerge [24,49], here the spectral peaks continue to exhibit an adiabatic growth and temporal narrowing even over long-term evolution after the spectral gradient catastrophe [26]. In order to illustrate a ‘solitonic DSW’ in the framework of integrable reduced models, we will now consider a slightly modified configuration of the system.

2.3.3. Benjamin–Ono kinetic equation

We consider here the regime in which the random wave evolves in the presence of a significant background spectral noise, $n_\omega(z) = n_0 + \tilde{n}_\omega(z)$. Indeed, this regime is interesting because the corresponding SID-KE recovers the integrable BO equation [26]. Considering a multi-scale expansion with $\tilde{n}_\omega(z) \sim n_0/\tau_R$ in Eq. (4), one obtains:

$$\tau_R^2 \partial_z \tilde{n}_\omega - (1 + \eta^2) n_0 \partial_\omega \tilde{n}_\omega = (1 + \eta^2) \left(\tilde{n}_\omega \partial_\omega \tilde{n}_\omega - \frac{1}{\tau_R} n_0 \mathcal{H} \partial_\omega^2 \tilde{n}_\omega \right). \quad (5)$$

The second term on the lhs can be removed by means of a change of Galilean reference frame in frequency space, so that Eq. (5) recovers the integrable BO equation, which provides here the deterministic description of the spectral dynamics of incoherent shocks. We illustrate incoherent DSWs starting either from a ‘bright’ or a ‘dark’ initial condition superimposed on the spectral background noise. For a bright initial condition (positive initial data vanishing at infinity) the random wave develops an incoherent ‘solitonic DSW’, where the singularity is eventually regularized by the formation of (incoherent) BO solitons [49]. Fig. 1 reports a typical spectral evolution of the random wave, in which the NLS simulation is compared to those of the WLT kinetic equation (2) and the reduced BO equation (5).

On the other hand, we report in Fig. 2 the evolution of an initial dark perturbation (spectral hole) on a continuous background: The spectral evolution is characterized by an expansion (rarefaction) wave on the leading edge and a gradient catastrophe on the trailing edge, which is regularized by an expanding dispersive wave train. We remark that in all cases analyzed in the weakly nonlinear regime, we always obtained a quantitative agreement between

the simulations of the stochastic NLS equation (1), WLT equation (2) and corresponding reduced SID-KEs (4)–(5), without using adjustable parameters. Note that the initial random waves in the NLS equation (1) have been generated by considering a Gaussian spectrum with δ -correlated spectral phases (see [26] for more details on the simulations).

3. Spatial domain: Collective incoherent shock waves

3.1. Spatial nonlocal NLS equation

In this section we consider the spatial counterpart of the temporal NLS equation considered above. In the context of optics, such an NLS equation models the transverse spatial evolution of an optical beam that propagates in a material featured by a nonlocal nonlinear response, e.g., thermal media [18], nematic liquid crystals [60,36], or glasses [61,62]. In this framework, the impact of nonlocality on the dynamics of nonlocal nonlinear waves has been investigated in different settings [63,64]. From a broader perspective, nonlocal nonlinearities are found in several physical systems, among which we may quote dipolar Bose–Einstein condensates [65], roton excitations in superfluids [66], atomic vapors [67], or plasmas [51]. The evolution of the field can be modeled by the following generic form of the defocusing NLS equation:

$$i\partial_z \psi = -\frac{1}{2} \partial_{xx} \psi + \psi \int U(x-x') |\psi|^2(x', z) dx', \quad (6)$$

where $U(x)$ is the nonlocal response function, whose typical width, say σ , denotes the nonlocal range of the interaction. In a way similar to the temporal case Eq. (1), we normalized the problem with respect to the healing length $\Lambda = \sqrt{\alpha L_{nl}}$, where α is the diffraction coefficient, $L_{nl} = 1/(\gamma\rho)$ the nonlinear length, γ the nonlinear coefficient, and ρ the wave intensity. For definiteness, we remind that the dimensional variables can be recovered through the substitution $\psi \rightarrow \psi \sqrt{\rho}$, $x \rightarrow x\Lambda$, $z \rightarrow zL_{nl}$ ($\rho = \mathcal{N}/L = L^{-1} \int_0^L |\psi|^2 dx = 1$, where L is the spatial numerical window). Note the presence of the factor (1/2) in front of the linear dispersion term in (6) which will prove convenient for the subsequent analysis. With this normalization, the nonlocal range (σ) and the correlation length (λ_c) are in units of Λ . In addition to the total ‘power’ of the field, $\mathcal{N} = \int |\psi|^2 dx$, we remind that the NLS equation (6) conserves the Hamiltonian, $\mathcal{H} = \mathcal{E} + \mathcal{U}$, which has a linear contribution $\mathcal{E}(z) = \frac{1}{2} \int |\partial_x \psi|^2(x, z) dx$, and a nonlinear contribution, $\mathcal{U}(z) = \frac{1}{2} \iint |\psi|^2(x, z) U(x-x') |\psi|^2(x', z) dx dx'$. In the numerical simulations we consider periodic boundary conditions in x space and assume the response function $U(x)$ Gaussian-shaped, of the form $U(x) = (2\pi\sigma^2)^{-1/2} \exp[-x^2/(2\sigma^2)]$.

3.2. Local vs nonlocal regimes

At variance with spectral incoherent shocks discussed above in Section 2, the development of incoherent shock singularities considered in this section requires a strongly nonlinear regime, as it is usual for conventional coherent shock waves [1]. Note that the requirement of a strong nonlinear interaction will become apparent below in the framework of the Vlasov approach. In the recent work [27], we considered the formation of incoherent shocks starting from an initially localized random wave that decays to zero over a length scale of the same order as the nonlocal nonlinear range, σ . Here, we consider an initial random wave that exhibits fluctuations that are homogeneous in space, except for the presence of a dip in its spatial envelope profile of the intensity, whose width is of the same order as the nonlocal nonlinear range, σ . The presence of such a hole in the intensity envelope will be

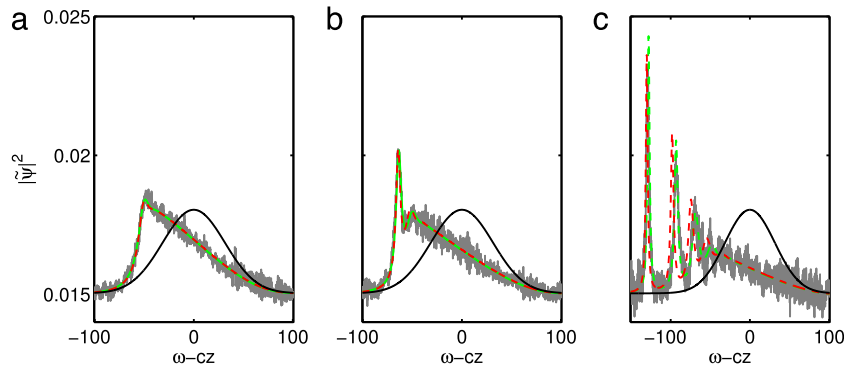


Fig. 1. Spectral incoherent DSWs in the ‘solitonic’ regime: Numerical simulation of the NLS equation (1) (with a damped harmonic oscillator response for $R(t)$), in the presence of a spectral background noise: The stochastic spectrum $|\tilde{\psi}|^2(\omega, z)$ develops a DSW at $z \simeq 2 \times 10^5$ ($\tau_R = 5, s = 1, \eta = 1$): $z = 2 \times 10^5$ (a), $z = 3 \times 10^5$ (b), $z = 7 \times 10^5$ (c). NLS result (gray) is compared with WLT kinetic equation (2) (green), and the reduced BO kinetic equation (5) (dashed-red). The initial condition is in solid black. (For interpretation of the references to color in this figure legend, the reader is referred to the web version of this article.)

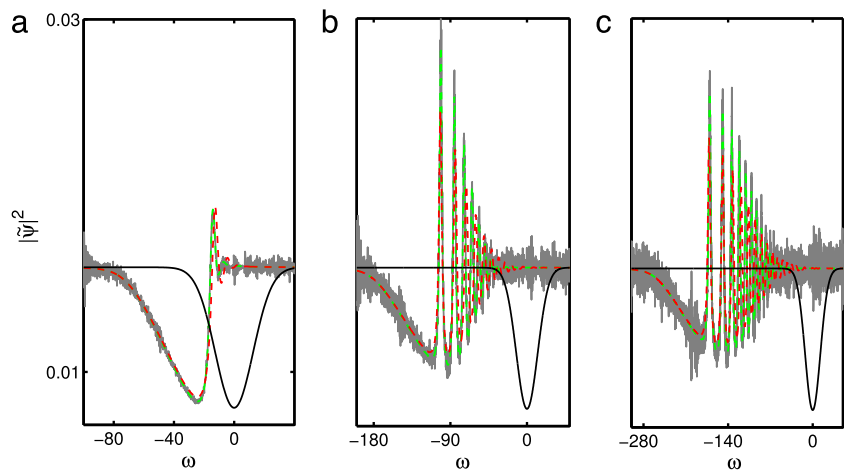


Fig. 2. Spectral incoherent DSWs in the ‘non-solitonic’ regime: The shock is regularized by the formation of an expanding wave train (same as in Fig. 1, except that the DSW is generated from a dark-like input). Numerical simulation of the NLS equation (1) with a damped harmonic oscillator response: The stochastic spectrum $|\tilde{\psi}|^2(\omega, z)$ develops a DSW at $z \simeq 5000$ ($\tau_R = 2, s = 1, \eta = 1$): $z = 6 \times 10^3$ (a), $z = 2 \times 10^4$ (b), $z = 3 \times 10^4$ (c). NLS simulations (gray) are compared with WLT kinetic equation (2) (green), and BO kinetic equation (5) (dashed-red). The initial condition is in solid black. (For interpretation of the references to color in this figure legend, the reader is referred to the web version of this article.)

shown to change in a deep way the nature of the incoherent shock as well as the corresponding long-term regularization of the singularity.

In the following we thus consider an initial random wave, $\psi_0(x) = \psi(x, z = 0)$, in the strong nonlinear regime, $\mathcal{U}_0 \gg \mathcal{E}_0$, where \mathcal{U}_0 and \mathcal{E}_0 refer to the initial values of the energies at $z = 0$. Note that this condition is analogous to $\lambda_c^0 \gg 1$ ($\lambda_c^0 \gg \Lambda$ in dimensional units), where λ_c^0 is the initial coherence length of the random wave, $\psi_0(x)$. In this regime, we now compare the case of a quasi-local (short-range) interaction, $\sigma \sim 1$, with a highly nonlocal (long-range) interaction, $\sigma \gg 1$ (we remind that σ is in units of Λ). For $\sigma \sim 1$, the random field leads to the formation of several coherent DSWs. In spite of the complexity of this dynamics, at a qualitative level it can be interpreted by remarking that since $\lambda_c^0 \gg 1$, every individual fluctuation evolves independently of each other, and thus develops its own DSW, as illustrated in the zoom of Fig. 3(b). As a result, in this quasi-local turbulent regime the incoherent wave develops singularities which are in essence small-scale coherent DSWs. Note that these ‘dispersive shocklets’ can be regarded as the conservative counterpart of viscous shocklets considered in high speed turbulent flows [68]. It is interesting to remark that, although this shocklets regime occurs in the presence of dispersion ($\omega(k) = k^2/2$ from the linearized NLS equation), it exhibits some interesting connections with a long-standing challenging issue of weakly dispersive acoustic-like wave turbulence [69], a feature commented in Ref. [27].

This physical picture changes in a dramatic way in the highly nonlocal (long-range) regime, $\sigma \gg 1$. This is illustrated in Fig. 3(c)–(d), which shows the evolution of the field starting from the same initial condition ($\psi_0(x)$) as in the quasi-local regime. The main difference is that in the highly nonlocal regime the fluctuations of the incoherent wave exhibit a global collective behavior, which is responsible for the formation of a large-scale incoherent shock wave of a fundamental different nature, since it is now the incoherent wave as a whole which develops a shock. The analysis developed below will reveal that the momentum of the random wave exhibits a gradient catastrophe shock singularity toward the dark notch center ($x = 0$), which is characterized by a dramatic degradation of the coherence of the random wave at the shock point (see the zoom in Fig. 3(d)). In order to analyze the properties of this incoherent shock, it proves convenient to study the evolution of the spectrogram (i.e., local spectrum of the random wave) in the general framework of the long-range Vlasov formalism.

3.3. Long-range Vlasov equation

The long-range Vlasov equation can be derived within the general framework of the wave turbulence theory [29–31,33]. In this respect, it is important to note that, in the long-range regime of interaction, resonant four-wave interactions underlying

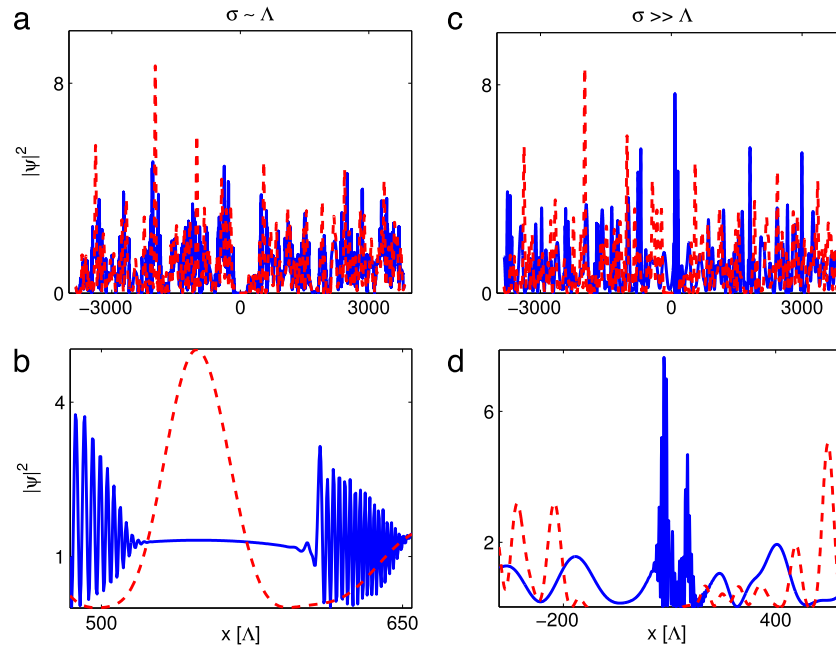


Fig. 3. Spatial incoherent shock waves: Local (left column) vs nonlocal (right column) regimes. Numerical simulations of the NLS equation (6) starting from the same initial condition, $|\psi|^2(x, z = 0)$ (dashed red lines): (a) In the quasi-local regime $\sigma = 2$, each individual fluctuation of the random wave develops a coherent DSW, as illustrated in the zoom (b), which reports a zoom of $|\psi|^2(x, z = 20)$ (blue line). (c) In the highly nonlocal regime $\sigma = 200$, the analysis reveals that the random wave as a whole develops a collective incoherent shock nearby the initial hole at $x = 0$, see the zoom in (d) which reports $|\psi|^2(x, z = 350)$ (blue line). (For interpretation of the references to color in this figure legend, the reader is referred to the web version of this article.)

the NLS equation (6) are described by a wave turbulence collision term which can be shown to be of higher order with respect to the transport Vlasov terms (see Ref. [27] for more details). It remarkably turns out that the collisionless long-range Vlasov equation provides an accurate description of the highly nonlocal regime of the random wave. More specifically, the long-range Vlasov equation governs the evolution of the *averaged* local spectrum of the wave [50,35]:

$$\partial_z n_k(x, z) + \partial_k \Omega_k(x, z) \partial_x n_k(x, z) - \partial_x \Omega_k(x, z) \partial_k n_k(x, z) = 0, \quad (7)$$

where $n_k(x, z)$ denotes the ‘local’ spectrum in the sense that it depends on the spatial position, x . It is defined as the Wigner-like transform of the correlation function, $n_k(x, z) = \int B(x, \xi, z) \exp(-ik\xi) d\xi$ with $B(x, \xi, z) = \langle \psi(x + \xi/2, z) \psi^*(x - \xi/2, z) \rangle$ and $\langle \cdot \rangle$ denotes an average over the realizations [35]. The generalized dispersion relation in (7) is $\Omega_k(x, z) = \omega(k) + V(x, z)$, where $V(x, z) = \frac{1}{2\pi} \int U(x - x') N(x', z) dx'$ is the effective potential, $N(x, z) = \int n_k(x, z) dk$ is the envelope intensity, and $\omega(k) = k^2/2$ (with our normalization, $\mathcal{N} = (2\pi)^{-1} \int N(x, z) dx = L$).

Note that a detailed comparative analysis of NLS and Vlasov simulations revealed a quantitative agreement in the long-range regime [70], even in the strong nonlinear regime of interaction [27]. Although to our knowledge there is no rigorous proof of this remarkable fact, it can be interpreted on the basis of statistical arguments similar to those discussed in Ref. [71], in which it was shown that, owing to a highly nonlocal response, the statistics of the random wave turns out to be Gaussian. Then contrarily to a conventional Vlasov equation, whose validity is constrained by the assumptions of (i) weakly nonlinear interaction and (ii) quasi-homogeneous statistics, the long-range Vlasov equation provides an ‘exact’ statistical description of the random wave in the highly nonlocal regime [50]. Note that this property is corroborated by the fact that the Vlasov equation considered here is formally analogous to that considered to study long-range interacting systems [55,56], where it has been proven that in the limit of an infinite number of particles the dynamics of mean-field Hamiltonian systems is governed by a long-range

Vlasov formalism (although the terminology ‘long-range’ used in [55,56] refers to genuine divergent spatial integrals of the nonlocal response function, while we consider here Gaussian or exponential-shaped response functions typically encountered in nonlinear optics).

3.4. Spectrogram hole formation

To gain physical insight into the incoherent shock singularity, we report here numerical simulations of both the NLS (6) and Vlasov (7) equations. Fig. 4 illustrates the evolution of the spectrograms in a relatively weak nonlinear regime of interaction, $\varepsilon_0/\mathcal{U}_0 \simeq 2.5$. We note in Fig. 4 that the initial line hole in the spectrogram is twisted during the propagation, a feature that can be intuitively interpreted on the basis of the particle analogy provided by the Vlasov formalism. We remind that the random wave is modeled by an ensemble of particles with the energy $\Omega_k(x, z) = \frac{1}{2}k^2 + V(x, z)$, so that the dynamics of a single particle is determined by the collective nonlinear potential induced by all other particles, $V(x, z)$. Because of the relatively large value of $\varepsilon_0/\mathcal{U}_0$, the random wave ‘contains’ particles whose velocity $v(k) = \partial_k \omega(k) = k$ is large enough to be only marginally affected by the nonlinear potential dip, $V(x)$. In this way the counter-streaming flows of particles with positive velocity ($v(k) > 0$ for $k > 0$) and negative velocity ($v(k) < 0$ for $k < 0$), lead to a twist of the line hole in phase space. This in turn leads to a homogenization process during the evolution, so that the intensity envelope relaxes during the propagation toward a homogeneous state, $N(x, z) \rightarrow N_0$ for large z . This effective damping of the initial hole perturbation in the intensity envelope is illustrated in Fig. 4(g)–(h). We remind that this irreversible process of relaxation occurs in a conservative Hamiltonian system. It is in fact analogous to the celebrated phenomenon of Landau damping [72], which results from a phase mixing homogenization process that occurs in phase space.

Let us note that, contrary to what has been reported in previous studies of incoherent dark solitons in slowly responding

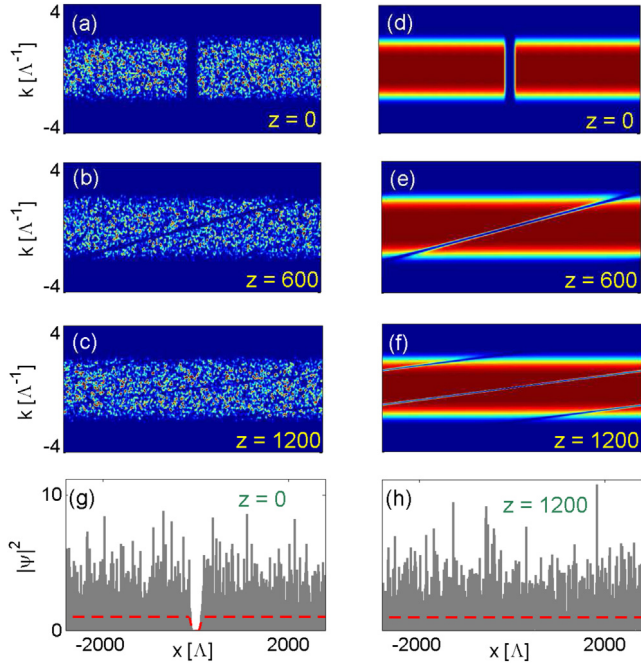


Fig. 4. Evolution of the spectrograms obtained by numerical simulations of the NLS equation (6) (left column: panels (a) to (c)) and Vlasov equation (7) (right column: panels (d) to (f)), in the weakly nonlinear regime, $\varepsilon_0/\mathcal{U}_0 \simeq 2.5$ ($\sigma = 200$). The initial line hole is twisted during the propagation, which leads to an irreversible evolution of the random wave toward the homogeneous state, as illustrated by the intensity profiles in NLS (plots of $|\psi|^2(x, z)$, gray) and Vlasov (plots of $N(x, z)/(2\pi)$, dashed red) for $z = 0$ (g), $z = 1200$ (h).

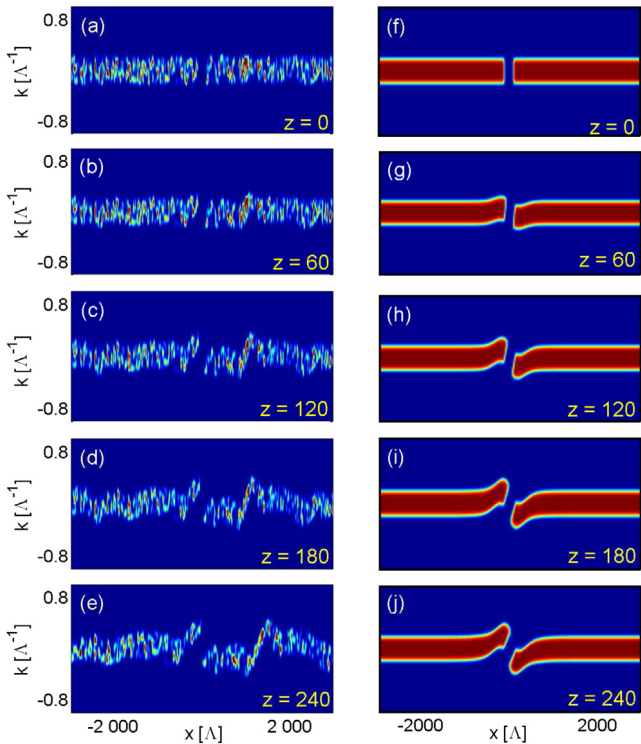


Fig. 5. Evolution of the spectrograms obtained by numerical simulations of the NLS equation (6) (left column) and Vlasov equation (7) (right column), in the strongly nonlinear interaction regime, $\varepsilon_0/\mathcal{U}_0 \simeq 0.024$ ($\sigma = 200$). The random wave exhibits a sudden spectral broadening nearby the initial line hole at $x = 0$, which takes place toward $k > 0$ ($k < 0$) for particles moving toward increasing (decreasing) values of x , subsequently leading to a shock singularity for the momentum of the opposing currents (see the evolution of $K(x, z)$ in Fig. 6).

photorefractive materials [73,74], here we verified that the introduction of a π -phase shift at the dark notch center ($x = 0$) does not play any role in the subsequent dynamics. This is consistent with the long-range Vlasov formalism (7), which does not keep trace of phase information effects.

The situation illustrated through Fig. 4 changes in a substantial way when the propagation of the random wave enters a strongly nonlinear regime of interaction, $\varepsilon_0/\mathcal{U}_0 \ll 1$. In this case the random wave essentially ‘contains’ low energetic particles, whose slow motion is thus deeply affected by the nonlinear potential. This leads to a completely different spectrogram dynamics, as illustrated in Fig. 5. By falling into the corresponding opposite fronts of the potential dip, the counter-propagating particles result to be strongly accelerated. This means that the random wave exhibits a sudden spectral broadening, which takes place toward $k > 0$ ($k < 0$) for particles moving toward increasing (decreasing) values of x , subsequently leading to a shock singularity for the momentum of the opposing currents (see Fig. 6). As a result of their nonlinear interaction, the strong accumulation of particles in the potential dip in turn modifies the self-induced potential, $V(x, z)$, which thus becomes flatter and subsequently double-well-shaped, as illustrated in Fig. 7 for $z \lesssim 600$. The counter-streaming particles then get trapped within the two distinct channels in the spectrogram, whose dynamics is still coupled by the long-range potential, which thus leads to a complex oscillatory spatio-temporal dynamics, see Fig. 7 for $z \gtrsim 600$. As a remarkable and unexpected result, this complex dynamics eventually leads to the spontaneous nucleation of a deep hole in the spectrogram. The term ‘nucleation’ is inspired by the fact that, once generated, the spectrogram hole proves extremely robust and is thus preserved for arbitrarily long propagation distances in z up to random shifts in the x direction, as illustrated in Figs. 7–8.

In the following we first show that the first mechanism leading to the generation of the spectrogram hole is a shock singularity, next we show that the robustness of such a phase space hole can be interpreted in the light of an incoherent dark soliton solution.

3.5. Incoherent shock singularity

The previous numerical analysis revealed that the formation of the spectrogram hole in phase-space (x, k) takes place into the strong nonlinear regime of interaction, which is characterized by a very narrow spectral dynamics. Accordingly, the spectrogram dynamics can be described by means of singular solutions of the Vlasov equation [27], $n_k(x, z) = N(x, z)\delta(k - K(x, z))$, which leads to the following hydrodynamic-like model governing the evolutions of the intensity envelope, $N(x, z)$, and momentum, $K(x, z)$:

$$\partial_z N + \partial_x(NK) = 0, \quad (8)$$

$$\partial_z K + K\partial_x K + \partial_x V = 0, \quad (9)$$

where we remind that the self-consistent potential reads, $V(x, z) = \frac{1}{2\pi} \int U(x - y)N(y, z)dy$. Let us note that the ‘hydrodynamic’ model equations (8)–(9) recover the one-dimensional shallow-water equations under the substitution $V(r, z) \rightarrow N(r, z)/(2\pi)$ [1]. We will see in the following that the existence of a long-range interaction mediated by the convolution with the nonlocal potential, $U(x)$, changes the dynamics in a substantial fashion.

Starting from $K(x, z = 0) = 0$, the ‘spectrogram’ $K(x, z)$ is initially driven by the last nonlinear term in (9), while the Burgers-like (second) term of (9) subsequently leads to the gradient catastrophe of $K(x, z)$ toward the point $x = 0$ – the particles with a positive (negative) velocity accumulate nearby $x = 0^-$ ($x = 0^+$). The finite ‘time’ (distance, z) shock singularity

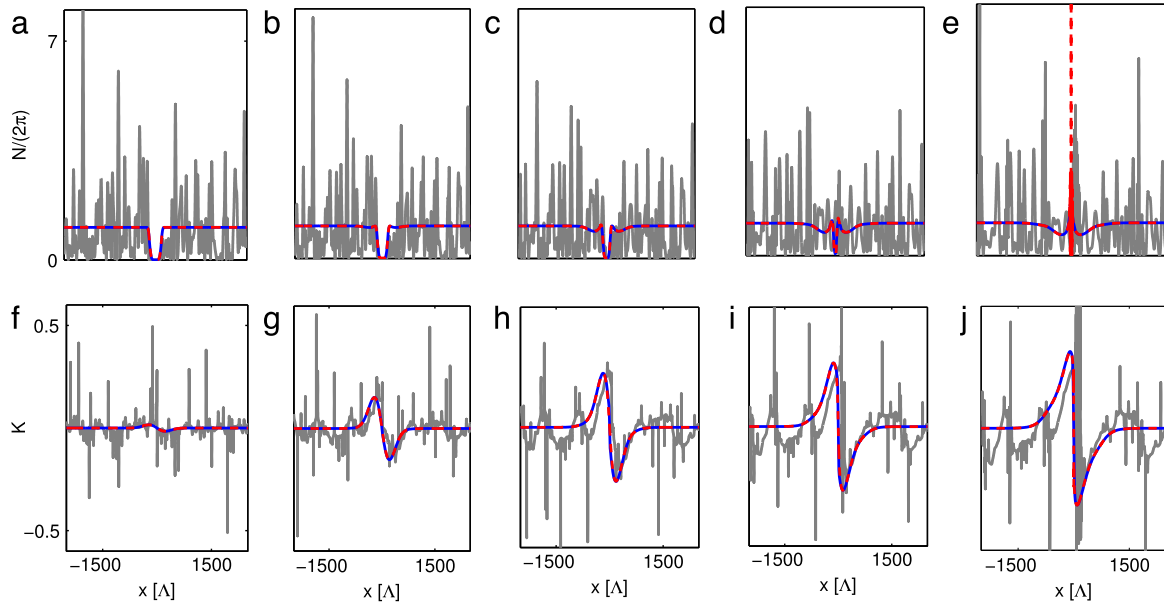


Fig. 6. Incoherent shock singularity: Evolutions of $N(x, z)$ (1st row) and $K(x, z)$ (2nd row) obtained by simulations of NLSE (6) (gray), Vlasov equation (7) (blue), ‘hydrodynamic’ model (8)–(9) (dashed red), $z = 10, 100, 200, 300, 380$, from left to right ($\sigma = 200$). The momenta are evaluated as follows: for NLSE, $K_{\text{NLS}}(x, z) = \frac{2\pi}{N} \Im(\psi^* \partial_x \psi)$, for the Vlasov equation, $K_{\text{Vlas}}(x, z) = \frac{1}{N} \int kn_k dk$. The comparison between NLS, Vlasov and ‘hydrodynamic’ model simulations has been performed without using adjustable parameters. (For interpretation of the references to color in this figure legend, the reader is referred to the web version of this article.)

of $K(x, z)$ is responsible for a collapse singularity of the intensity envelope $N(x = 0, z)$, see Fig. 6. These singular behaviors can be described theoretically by solving Eqs. (8)–(9) by the method of the characteristics [75]. We define $w(z) = K(X(z), z)$, $\tau(z) = \partial_x K(X(z), z)$, $\xi(z) = \partial_x K(X(z), z)$, and $\phi(z) = N(X(z), z)$, which can be shown to satisfy

$$\dot{X}(z) = w(z), \quad X(0) = x_0, \quad (10)$$

$$\dot{w}(z) = \tau(z) + w(z)\xi(z), \quad w(0) = 0, \quad (11)$$

$$\dot{\tau}(z) = -\partial_{xx}^2 V(X(z), z) - \xi(z)\tau(z), \quad \tau(0) = -\partial_x V(x_0, 0) \quad (12)$$

$$\dot{\xi}(z) = -\partial_x^2 V(X(z), z) - \xi^2(z), \quad \xi(0) = 0, \quad (13)$$

$$\dot{\phi}(z) = -\xi(z)\phi(z), \quad \phi(0) = N(x_0, 0), \quad (14)$$

where the dots denote the ‘temporal’ derivatives, $\dot{X}(z) = \partial_z X(z)$. Note that Eq. (14) is obtained by writing (8) along the characteristic, $X(z)$. Observing that $V(x, z)$ and its spatial derivatives are uniformly bounded, it can be shown that $\xi(z)$ and $\phi(z)$ exhibit a finite time blow-up singularity. More specifically, we can consider the singular behaviors along the characteristic, $X(z) = 0$, with $w(z) = 0$, $\tau(z) = 0$:

– If σ is larger than the typical width of the initial hole in $N(x_0, 0)$, then we can approximate $\partial_x^2 V(0, z) \simeq -\partial_x^2 U(0) \tilde{\mathcal{N}}$, with $\tilde{\mathcal{N}} = \frac{1}{2\pi} \int N_0 - N(x, 0) dx$. Accordingly, the equations for ξ and ϕ satisfy $\dot{\xi} = -k_0^2 - \xi^2$, $\dot{\phi} = -\xi\phi$, with $k_0^2 = -\partial_x^2 U(0) \tilde{\mathcal{N}} > 0$, which gives the solutions:

$$N(0, z) = \frac{N(0, 0)}{\cos(k_0 z)}, \quad \partial_x K(0, z) = -k_0 \tan(k_0 z). \quad (15)$$

This shows that the intensity envelope and the gradient of the momentum both exhibit a blow up as $1/(z - z_\infty)$ with $z_\infty = \pi/(2k_0)$.

– If σ is of the same order as the width of the dip $N_0 - N(x, 0)$, we remark that we always have $c_- \leq \partial_x^2 V(0, z) \leq c_+$, where $c_\pm = \tilde{\mathcal{N}} m_\pm$ with $m_+ = \max(\partial_x^2 U(x))$ and $m_- = \min(\partial_x^2 U(x))$. Therefore $\dot{\xi} \leq -c_- - \xi^2$, so that whenever $\xi(z)$ reaches $-\sqrt{-c_-}$, then $\xi(z)$ also blows up in finite ‘time’ as $-1/(z - z_\infty)$.

Remarking that $\phi(z) = N(0, 0) \exp(-\int_0^z \xi(s) ds)$ from (14), we obtain the singular behaviors of $\xi(z)$ and $\phi(z)$ just before $z = z_\infty$:

$$N(0, z) \simeq \frac{1}{z_\infty - z}, \quad \partial_x K(0, z) \simeq \frac{-1}{z_\infty - z}. \quad (16)$$

It is important to note that the singular behaviors expressed by (16) are regularized by the NLS and Vlasov models. Indeed, the distribution $n_k(x, z)$ evolves in a two-dimensional phase-space (x, k) and can thus become ‘multi-valued’ beyond the shock point, as illustrated in Fig. 5(j) or in Fig. 7 for $z \gtrsim 300$. However, as discussed below in the concluding section, the derivation of reduced equations describing the regularization of the double shock-collapse singularity constitutes a difficult issue related to the long-standing problem of achieving a closure of the infinite hierarchy of equations that govern the evolutions of k -moments in transport-like kinetic equations [76]. We note in this respect that the wave turbulence theory establishes a closure in the *weakly nonlinear regime* [29–31,33], while the closure considered here concerns the opposite *strongly nonlinear regime*. Also note that in the context of self-gravitating systems, a weak diffusive effect has been introduced in a heuristic way to regularize the wave breaking shock singularity described by the inviscid Burgers equation, thus leading to the so-called ‘adhesion model’ [77], although so far no rigorous theory has been developed to justify such phenomenological approach [56].

We finally note that, at variance with shallow-water equations, which are hyperbolic equations and thus do not exhibit collapse singularities, here the collapse singularity of the intensity envelope in Eqs. (8)–(9) originates into the long-range nature of the interaction expressed by the convolution between the nonlocal potential, $U(x)$, and the intensity, $N(x, z)$.

3.6. Robustness of the spectrogram hole: Incoherent dark soliton states

The robustness of the spectrogram hole revealed by the numerical simulations in Figs. 7–8 can be interpreted in terms of incoherent dark soliton states. In the following we first consider

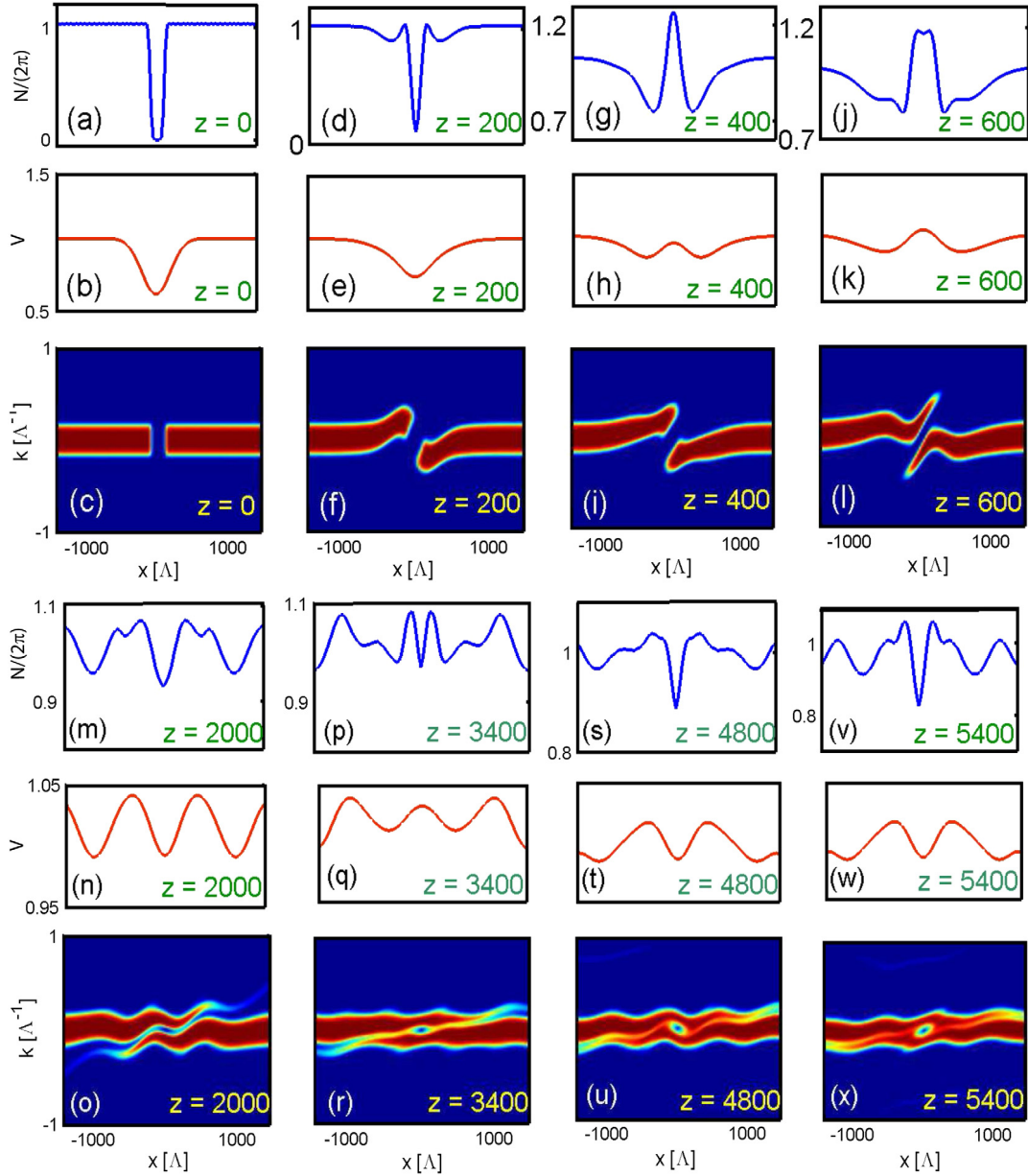


Fig. 7. Phase-space hole formation: Simulation of the long-range Vlasov equation (7) showing the evolution of the system well beyond the shock singularity. After a complex transient, a robust hole in the phase-space spectrogram is generated ($\varepsilon_0/U_0 \approx 0.018$, $\sigma = 200$). The rows show the evolutions during the propagation in z of the phase-space spectrogram $n_k(x, z)$ (3rd and 6th rows), and the corresponding evolutions of the intensity $N(x, z) = \int n_k(x, z) dk$ (1st and 4th rows), and self-consistent potential $V(x, z) = \frac{1}{2\pi} \int U(x - x') N(x', z) dx'$ (2nd and 5th rows).

a usual procedure used to derive non-homogeneous stationary solutions of Vlasov-like equations. This allows us to obtain a dark soliton state that exhibits an appropriate intensity profile of the random wave in real space. However this soliton solution is characterized by an underlying divergence of the spectrogram along some specific contour in phase-space, a feature which prevents us to connect the hole with a homogeneous background in phase-space. We circumvent this problem by deriving a different solution which is characterized by a stationary hole within a spectrogram that is otherwise approximately constant in phase-space.

3.7. Dark soliton solution without phase-space background

To derive an analytical dark soliton solution we remind an important observation originally pointed out in Ref. [78], namely

that a stationary solution of Vlasov-like equations can be expressed as an arbitrary function of the energy per particle, $\Omega_k(x) = \frac{1}{2}k^2 + V(x)$. Dark soliton states in the defocusing regime can be described as a consequence of a self-consistent self-trapping of the particles which results from their own induced self-consistent potential, in complete analogy with bright soliton states in the focusing regime [79,50] (also see Ref. [73] for dark incoherent optical solitons, and [80] for a review on the formation and dynamics of electrons and ion phase-space vortices in collisionless plasmas). In the defocusing case, the particles can be trapped by an effective potential provided that the corresponding (averaged) intensity exhibits a dip in its spatial profile, as illustrated in Fig. 9(b). In this case, it proves convenient to shift the energy by $V_0 = N_0/(2\pi)$ by defining, $h = \frac{1}{2}k^2 + V(x) - V_0$. Now the idea of the method is to argue that the ‘particles’ that constitute the dark soliton are trapped by the self-consistent potential, $V(x) - V_0 \leq 0$, provided

that their energy is negative, $h \leq 0$, see Fig. 9. This determines a specific interval of momenta for the trapped particles, $-k_c \leq k \leq k_c$, where $k_c = \sqrt{-2(V - V_0)}$. The spectrogram of the stationary solution thus reads $n_k^{st}(x) = \eta^{st}(\frac{1}{2}k^2 + V(x) - V_0)$, while the corresponding intensity profile is $N(x) = \int_{-k_c}^{+k_c} n_k^{st}(x) dk$. By means of a change of variable, this integral can be expressed in the form of a Fredholm equation

$$N = \int_{V-V_0}^0 \frac{\eta^{st}(h)}{\sqrt{(h - V + V_0)/2}} dh. \quad (17)$$

With $U(x) = (2\pi\sigma^2)^{-1/2} \exp[-x^2/(2\sigma^2)]$, this equation admits the following analytical solution:

$$N(x) = N_0 (1 - d \exp(-x^2/(2\sigma_N^2))) \quad (18)$$

$$\eta^{st}(h) = \left(\frac{N_0}{\pi\sqrt{-2h}} - Q_\alpha (-h)^{\frac{1}{\alpha}-\frac{1}{2}} \right) H(-h), \quad (19)$$

$$Q_\alpha = \frac{\Gamma(1 + \alpha^{-1}) (2\pi)^{\frac{1}{\alpha}-\frac{1}{2}}}{\Gamma(1/2 + \alpha^{-1}) \alpha^{\frac{1}{2\alpha}} N_0^{\frac{1}{\alpha}-1} d^{\frac{1}{\alpha}-1}} \quad (20)$$

$$\alpha = \frac{1}{1 + \sigma^2/\sigma_N^2} \quad (21)$$

where $N_0 = 2\pi/(1 - \sqrt{2\pi}d\sigma_N/L)$, $\Gamma(x)$ is the Gamma function and the effective potential is $V(x) = V_0(1 - d\sqrt{\alpha} \exp(-\alpha x^2/(2\sigma_N^2)))$. The solution is characterized by a contour in the spectrogram defined by the lines:

$$k_c(x) = \pm\sqrt{-2(V(x) - V_0)}, \quad (22)$$

as illustrated in Fig. 9. It is important to note that along this contour (22) the solution $n_k^{st}(x)$ exhibits a divergence in phase-space, while the solution is not defined for $|k| \geq k_c(x)$. Note however that the solution (19) is self-consistent, in the sense that it verifies $\int_{-k_c}^{+k_c} n_k^{st}(x) dk = N(x)$. Also note that in the limit $\sigma \rightarrow 0$, i.e., $\alpha = 1$, the dark soliton solution recovers the form of the solution obtained in the limit of a local interaction, $U(x) \rightarrow \delta(x)$ [79].

3.8. Dark soliton solution with homogeneous phase-space background

The dark soliton solution of the Vlasov equation given through Eqs. (18)–(21) exhibits a major drawback: The divergence of the solution along the contour $k_c(x)$ in phase-space [Eq. (22)] prevents the connection of the hole with a homogeneous background of the spectrogram in phase-space. Then despite the fact that the spatial intensity profile of the solution exhibits the usual appropriate dark soliton shape (see Fig. 9(b)), the underlying spectrogram does not exhibit a homogeneous background and thus strongly differs from the phase-space holes states typically obtained from simulations of the Vlasov equation, see Fig. 7.

In this section we derive a dark soliton solution characterized by a spectrogram hole with a homogeneous background in phase-space, with constant amplitude n_0 . We thus consider a solution of the form: $n_k(x, z) = n_0 - \tilde{n}_k(x, z)$. By substitution into the defocusing Vlasov equation (7), one readily sees that $\tilde{n}_k(x, z)$ verifies the following focusing version of the Vlasov equation:

$$\partial_z \tilde{n}_k + k \partial_x \tilde{n}_k + \partial_x \tilde{V} \partial_k \tilde{n}_k = 0, \quad (23)$$

where $\tilde{V}(x, z) = \frac{1}{2\pi} \int U(x-y) \tilde{N}(y, z) dy$, with $\tilde{N}(x, z) = \int \tilde{n}_k(x) dk$. Hence, in the defocusing regime, the spectrogram hole $\tilde{n}_k(x, z)$ results to be governed by an effective focusing Vlasov equation. Now, in the focusing regime, the particles $\tilde{n}_k^{st}(x)$ that constitute the soliton are trapped by the self-consistent potential, $-\tilde{V}(x)$,

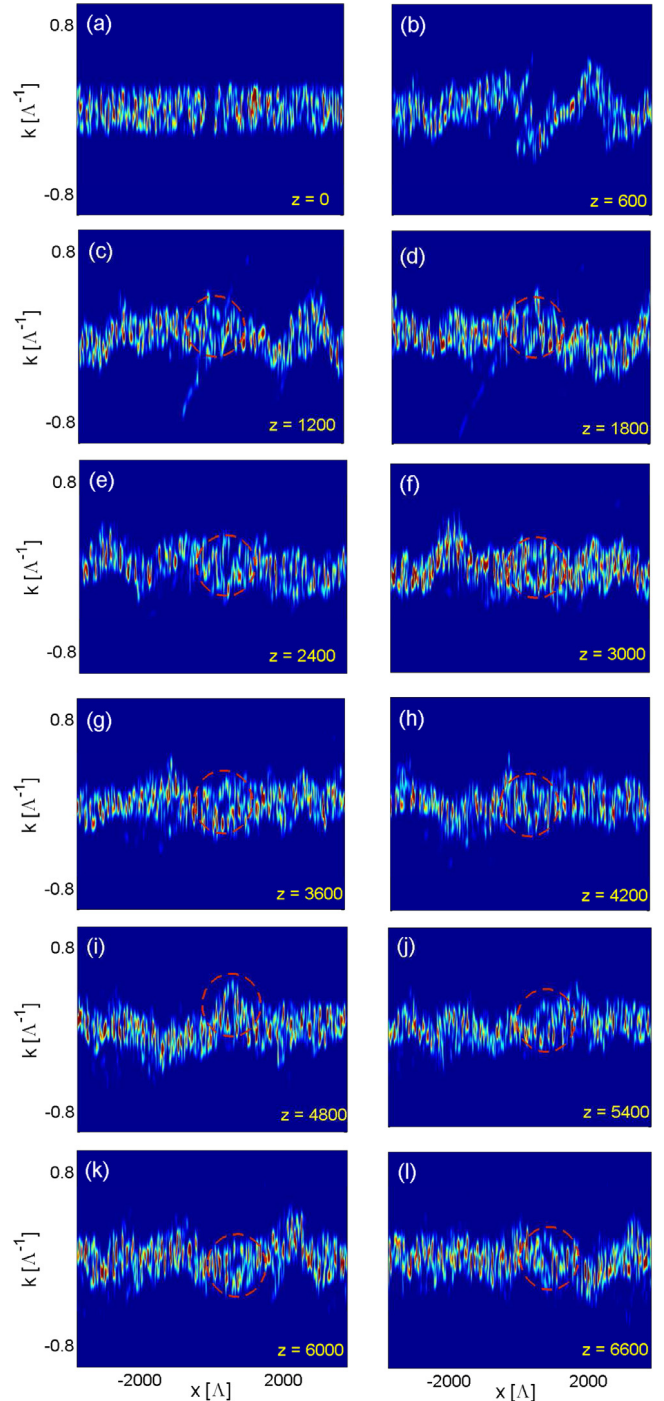


Fig. 8. Phase-space hole formation: Evolution of the spectrogram obtained by simulation of the NLS equation (6) showing the formation of a hole in the phase-space well beyond the shock singularity ($\epsilon_0/\mathcal{U}_0 \simeq 0.024$, $\sigma = 200$). Note that, contrary to deterministic Vlasov simulations, NLS simulations are inherently stochastic and fluctuations may lead to a shift in the spatial position of the phase-space hole.

provided that their energy is negative, $\tilde{h} = \frac{1}{2}k^2 - \tilde{V}(x) \leq 0$. Proceeding as in the previous section, we can exhibit the following stationary solution with background

$$\eta^{st-bg}(\tilde{h}) = n_0 - \tilde{\eta}^{st}(\tilde{h}), \quad (24)$$

where $\tilde{\eta}^{st}(\tilde{h})$ has compact support in k and is rapidly decaying in x :

$$\tilde{N}(x) = \frac{\sqrt{2\pi} \tilde{\mathcal{N}}}{\sigma_N} \exp\left(-\frac{x^2}{2\sigma_N^2}\right), \quad (25)$$

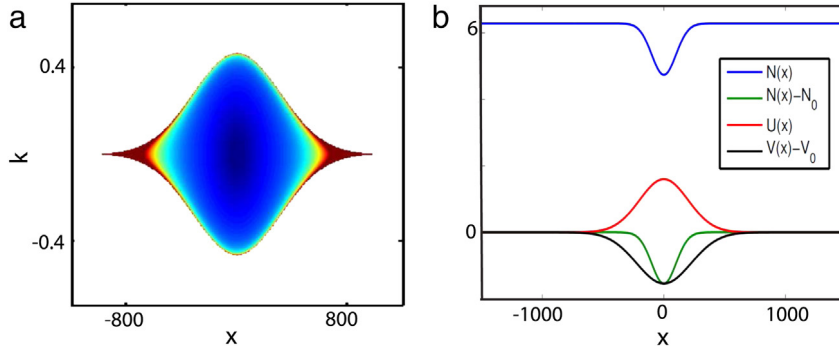


Fig. 9. Dark soliton solution without phase-space background [Eqs. (18)–(21)]: (a) Plot of the dark soliton solution of the Vlasov equation, $n_k^{st}(x)$, given by Eq. (19) for $\sigma = 200$, $\sigma_N = 100$ and $n_{k=0}^{st}(x=0) = 0$. Note that the solution diverges on the contour given by $k_c(x)$ in Eq. (22) and it is not defined for $|k| > k_c(x)$. (b) Corresponding plots of the intensity profile $N(x)$ (blue line), nonlocal potential $U(x)$ (red line), and self-consistent trapping potential $V(x) - V_0$ (dark line), given by the dark soliton solution ($\sigma = 200$, $\sigma_N = 100$). A dark soliton forms when the random wave induces an effective self-consistent self-trapping potential $\tilde{V}(x) = V(x) - V_0 < 0$ owing to a defocusing nonlinearity (for visibility reasons, $U(x)$ has been multiplied by a factor 800, $V(x) - V_0$ by a factor 14). (For interpretation of the references to color in this figure legend, the reader is referred to the web version of this article.)

$$\tilde{\eta}^{st}(\tilde{h}) = \tilde{Q}_\alpha (-\tilde{h})^{\frac{1}{\alpha} - \frac{1}{2}} H(-\tilde{h}), \quad (26)$$

$$\tilde{Q}_\alpha = \frac{\Gamma(1 + \frac{1}{\alpha})(2\pi)^{\frac{1}{2\alpha}}(\sigma^2 + \sigma_N^2)^{\frac{1}{2\alpha}} \tilde{\mathcal{N}}^{1 - \frac{1}{\alpha}}}{\Gamma(\frac{1}{2} + \frac{1}{\alpha}) \sigma_N}, \quad (27)$$

where the parameter α is still given by Eq. (21). The corresponding self-consistent potential reads $\tilde{V}(x) = (\tilde{\mathcal{N}}\sqrt{\alpha}/(\sqrt{2\pi}\sigma_N)) \exp(-\alpha x^2/(2\sigma_N^2))$. The compact support in k of solution $\tilde{n}_k^{st}(x)$ originates in the condition of particle trapping underlying the dark soliton state. More precisely, considering that $\sqrt{2\pi}\tilde{\mathcal{N}}/\sigma_N = N_0 d$, then $V(x) - V_0 = -\tilde{V}(x)$, so that the particle trapping condition is the same as that considered above for the solution (18)–(21), namely $h = \tilde{h} \leq 0$, or $|k| \leq k_c(x) = \sqrt{2\tilde{V}(x)}$. There is however a fundamental difference which distinguishes the two soliton solutions: *In contrast to the previous solution Eqs. (18)–(21), here the spectrogram hole (24) is connected to a homogeneous constant phase-space background of amplitude n_0 .*

The dark soliton solution is characterized by two free parameters, the spatial width σ_N and the mass $\tilde{\mathcal{N}}$. However, this solution is acceptable only if $\tilde{n}_k^{st}(x) \leq n_0$ for all (k, x) , that is to say, provided $\tilde{n}_{k=0}^{st}(x=0) \leq n_0$. In this respect, it is interesting to note that $n_k^{st-bg}(x)$ can vanish at the center of the spectrogram, $k = x = 0$, which gives a deep hole in phase-space since then $n_{k=0}(x=0, z) = 0$. In this case the free parameters σ_N and $\tilde{\mathcal{N}}$ get linked. The dark soliton solution then takes the form

$$n_k^{st-bg}(x) = n_0 \left(1 - \left[\exp\left(-\frac{\alpha x^2}{2\sigma_N^2}\right) - \frac{\pi}{\alpha n_0^2} \frac{\Gamma^2(1 + \frac{1}{\alpha})}{\Gamma^2(\frac{1}{2} + \frac{1}{\alpha})} k^2 \right]^{\frac{1}{\alpha} - \frac{1}{2}} \right). \quad (28)$$

The width of the hole in x is σ_N and the width in k is $\alpha n_0/\sqrt{\pi}$ since $\frac{\Gamma^2(1 + \frac{1}{\alpha})}{\Gamma^2(\frac{1}{2} + \frac{1}{\alpha})} \sim \frac{1}{\alpha}$ for small α .

Note that, owing to the Galilean invariance of the Vlasov equation, the above dark soliton solution can be extended to a solution traveling with some ‘velocity’ w through the change of reference frame: $\xi = x + wz$, $\zeta = z$. The non-zero velocity solution reads, $n_k^{st-bg}(\xi) = n_0 - \tilde{n}_k^{st}(\xi)$, where $\tilde{n}_k^{st}(\xi) = \tilde{Q}_\alpha (\tilde{V}(\xi) - \frac{1}{2}(k + w)^2)^{\frac{1}{\alpha} - \frac{1}{2}}$ has a compact support in phase-space defined by $-\sqrt{2\tilde{V}(\xi)} - w \leq k \leq \sqrt{2\tilde{V}(\xi)} - w$. This solution shows that the phase-space hole can move in real space by acquiring some momentum, $k_0 = -w$, a property that can explain the shift in the position of the hole observed in NLS simulations in the presence of fluctuations, as illustrated in Fig. 8.

In the strongly nonlinear regime, the background spectrogram is rather narrow in k , with width $\Delta k < 1$, and its amplitude is

proportional to $1/\Delta k$. Therefore we must have $\alpha \sim \Delta k^2$, that is to say, $\sigma_N \sim \sigma \Delta k$, to ensure that the width of the hole in k is of order Δk and therefore fits into the background profile. This shows that the width in x of the phase-space hole is smaller than σ . Preliminary numerical simulations of the Vlasov equation confirm this important property of the dark soliton solution, at least for values of Δk large enough to generate holes within some relatively homogeneous phase-space background.

Finally note that the intensity profile of the dark soliton solution (28) can be written in the form, $N(x) = N_0(1 - d \exp(-x^2/(2\sigma_N^2)))$, with $d \simeq n_0^2 \Gamma^2(\frac{1}{2} + \frac{1}{\alpha}) \sqrt{\alpha}/(2\pi \Gamma^2(1 + \frac{1}{\alpha}))$, i.e., $d \sim \alpha^{3/2}$ for small α . We remark the interesting point that, despite that $n_k^{st-bg}(x)$ vanishes at the dark notch center, the resulting greyness of the dark soliton, d , rapidly decreases with the amount of nonlocality, as illustrated in Fig. 10(d) that reports d vs σ/σ_N . This reveals that, in spite of their robustness, the existence of deep holes in phase-space can hardly be identified through the analysis of the intensity profile in the usual real space.

4. Conclusion

4.1. Summary of the main results

On the basis of the NLS model equation, we have reported a unified presentation of different forms of incoherent shock waves in the presence of a long-range interaction, which can take place either in the temporal domain through a highly noninstantaneous nonlinearity, or in the spatial domain through a highly nonlocal nonlinearity. In the temporal domain, the system develops DSWs in the spectral dynamics of the random wave, despite the non-Hamiltonian structure of the NLS equation and the weakly nonlinear turbulent regime of interaction. These singularities are described in detail by a family of SID-KE, such as the integrable BO equation, which thus leads either to ‘solitonic’ or ‘non-solitonic’ spectral incoherent DSWs. In the spatial domain, the random wave exhibits a large scale global collective incoherent shock singularity that results from the long-range nature of the interaction. In spite of the Hamiltonian structure of the NLS model, the shock singularity is not characterized by the formation of a DSW. The regularization of the singularity takes place through a different process of coherence degradation that occurs near by the shock point. After a long transient characterized by a complex dynamics, the system is shown to nucleate a spectrogram hole in phase-space, which proves extremely robust and is thus preserved for arbitrarily long interaction times. We have interpreted such a robustness by deriving an analytical dark soliton solution of the

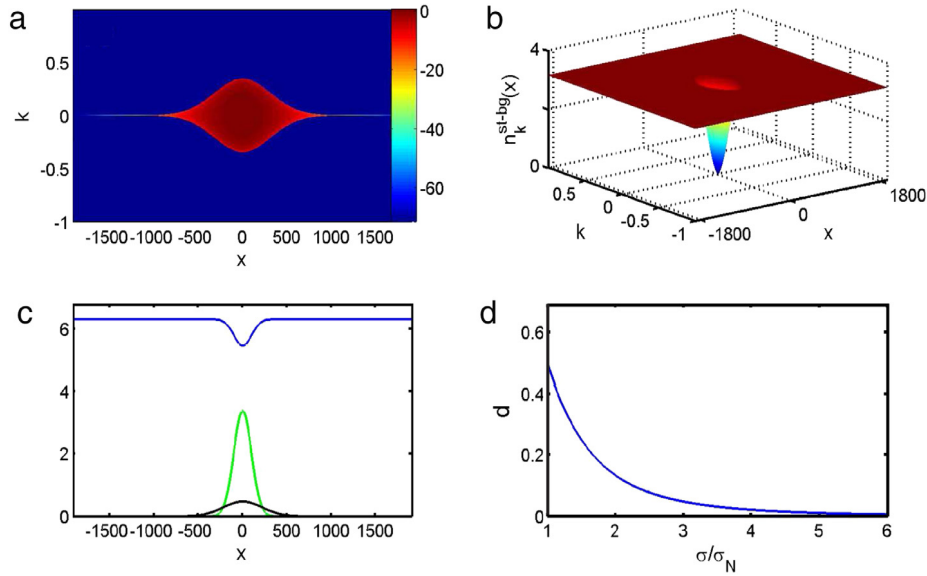


Fig. 10. Dark soliton solution with homogeneous phase-space background [Eqs. (24)–(27)]: (a) Plot of $\tilde{n}_k^{st}(x)$ given by Eq. (26): The solution is defined for $|k| \leq k_c(x)$, where $k_c(x) = \sqrt{2\tilde{V}(x)}$. (b) Plot of $n_k^{st-bg}(x)$ given by Eq. (28), which evidences the presence of a homogeneous constant background in phase-space, n_0 (note that $n_{k=0}^{st-bg}(x=0) = 0$). (c) Corresponding plots of the intensity dark soliton profile, $N(x) = N_0 - \tilde{N}(x)$ (blue line), $\tilde{N}(x)$ (green line), $\tilde{V}(x)$ (black line). (d) Dependence of the soliton greyness, d , with σ/σ_N , see the text: The greyness rapidly decreases with the amount of nonlocality, which makes incoherent dark solitons difficult to identify through their intensity profile $N(x)$, despite the fact that the spectrogram vanishes at the dark-notch center, $n_{k=0}^{st-bg}(x=0) = 0$, see panel (b) ($\sigma = 200$, $\sigma_N = 100$, the spatial and spectral windows are $L = 3840$, $K = 2$). (For interpretation of the references to color in this figure legend, the reader is referred to the web version of this article.)

long-range Vlasov equation, which is characterized by a stationary hole within a spectrogram that is otherwise constant in phase-space. The analysis reveals that the dark-soliton states are in some sense ‘hidden’ in the phase-space representation, in the sense that, despite the fact that the spectrogram vanishes at the dark notch center, $n_{k=0}(x=0, z) = 0$, they manifest themselves by means of a slight depletion in the intensity envelope of the random wave. Such a reduced greyness of incoherent dark soliton states makes their experimental observation extremely difficult, since an accurate measurement of the optical phase-space spectrogram still constitutes a delicate problem (see, e.g., [27]).

4.2. Regularization and closure issues

It would be important to develop a proper theoretical description of the mechanism underlying the regularization of the collective shock-collapse singularity discussed in the framework of a spatial long-range interaction. The derivation of reduced equations describing the regularization of the singularities is a difficult task which is related to a long-standing mathematical problem, namely achieving a closure of the infinite hierarchy of equations that govern the evolutions of k -moments in transport kinetic equations [76]. To comment on this problem, we remind that the ‘hydrodynamic model’ (8)–(9) accurately describes the dynamics up to the shock point, and thus breaks down beyond the finite ‘time’ singularities (16). It is important to note that this model refers to the lowest-order nonlinear closure of the hierarchy of k -moments equations for the long-range Vlasov equation. Then the natural way to go beyond this model would require a closure of the hierarchy at a higher order. In this respect, we note that in addition to the momentum $p(x, z) = \langle k \rangle(x, z)$, one can define higher-order k -moments as: $m_q(x, z) = N(x, z) \langle (k - p)^q \rangle$, where the average denotes $\langle \cdot \rangle(x, t) = N^{-1} \int \cdot n_k(x, t) dk$. From the long-range Vlasov equation, one obtains without approximations the following infinite hierarchy of moments equations:

$$\partial_z N + \partial_x(Np) = 0, \quad (29)$$

$$\partial_z p + p\partial_x p + \partial_x V = -\frac{1}{N} \partial_x m_2, \quad (30)$$

$$\begin{aligned} \partial_z m_q + \partial_x(pm_q + m_{q+1}) \\ = q \left(\frac{m_{q-1}}{N} \partial_x m_2 - m_q \partial_x p \right), \quad q \geq 2. \end{aligned} \quad (31)$$

The possibility of achieving a closure of the hierarchy (29)–(31) has been addressed in [27] through numerical simulations of the Vlasov equation. The study revealed that higher-order k -moments suddenly become all of the same order of magnitude nearby the shock singularity (16), which prevents an appropriate closure of the infinite hierarchy and thus a reduced description of the dynamics beyond the incoherent shock point. This indicates that a different approach should be developed to properly understand the mechanism of regularization of the double shock-collapse singularity (16) described by the hydrodynamic model (8)–(9). Work is in progress to address this issue.

Acknowledgments

A.P. and G.X. acknowledge support from the French National Research Agency (ANR-12-BS04-0011 OPTIROC) and the Labex ACTION (ANR-11-LABX-01-01) program. D.F. acknowledges support from European Research Council under the European Unions Seventh Framework Programme (FP/2007–2013)/ERC GA 306559 and EPSRC (UK, Grant EP/J00443X/1). S.T. acknowledges funding from Italian Ministry of Research (grant PRIN 2012BFNWZ2).

References

- [1] G.B. Whitham, *Linear and Nonlinear Waves*, Wiley, New York, 1974.
- [2] S.S. Miseev, R.Z. Sagdeev, *Plasma Phys.* 5 (1963) 43–47; R.Z. Sagdeev, in: Leontovich M.A. (Ed.), *Cooperative Phenomena and Shock Waves in Collisionless Plasmas*, in: *Review of Plasma Physics*, vol. 4, Consultants Bureau, New York, 1966, pp. 23–91.
- [3] N.J. Zabusky, M.D. Kruskal, *Phys. Rev. Lett.* 15 (1965) 240.
- [4] T.B. Benjamin, M.J. Lighthill, *Proc. R. Soc. Lond. Ser. A* 224 (1954) 448; D.H. Peregrine, *J. Fluid Mech.* 25 (1966) 321; R.S. Johnson, *Phys. Fluids* 15 (1972) 1693.
- [5] R.J. Taylor, D.R. Baker, H. Ikezi, *Phys. Rev. Lett.* 24 (1970) 206.
- [6] J.L. Hammack, H. Segur, *J. Fluid Mech.* 60 (1973) 769–799.

- [7] A. Gurevich, L. Pitaevskii, *Sov. Phys.—JETP* 38 (1974) 291.
- [8] G.B. Whitham, *Proc. R. Soc. Lond. Ser. A* 283 (1965) 238–261.
- [9] P.D. Lax, C.D. Levermore, *Proc. Natl. Acad. Sci. USA* 76 (1979) 3602.
- [10] B. Dubrovinn, *Comm. Math. Phys.* 267 (2006) 117–139;
B. Dubrovinn, *Amer. Math. Soc. Transl.* 224 (2008) 59–109;
T. Grava, C. Klein, *Physica D* 241 (2012) 2246–2264;
B. Dubrovinn, T. Grava, C. Klein, A. Moro, *J. Nonlinear Sci.* 25 (2015) 631–707.
- [11] G.A. El, *Chaos* 15 (2005) 1.
- [12] R.H. Clarke, R.K. Smith, D.G. Reid, *Mon. Weather Rev.* 109 (1981) 1726;
T.A. Coleman, K.R. Knupp, D. Herzmann, *Mon. Weather Rev.* 137 (2009) 495.
- [13] K.G. Lamb, Y. Liren, *J. Phys. Oceanogr.* 26 (1996) 2712;
G.A. El, R.H.J. Grimshaw, N.F. Smyth, *Phys. Fluids* 18 (2006) 027104.
- [14] H. Chanson, *Tidal Bores Aegir, Eagre, Mascaret, Proroca: Theory and Observations*, World Scientific, Singapore, 2012.
- [15] Z. Dutton, et al., *Science* 293 (2001) 663;
A.M. Kamchatnov, A. Gammal, R.A. Kraenkel, *Phys. Rev. A* 69 (2004) 063605;
M.A. Hoefer, et al., *Phys. Rev. A* 74 (2006) 023623;
J.J. Chang, P. Engels, M.A. Hoefer, *Phys. Rev. Lett.* 101 (2008) 170404;
R. Meppelink, et al., *Phys. Rev. A* 80 (2009) 043606;
M. Crosta, A. Fratalocchi, S. Trillo, *Phys. Rev. A* 85 (2012) 043607.
- [16] J.A. Joseph, et al., *Phys. Rev. Lett.* 106 (2011) 150401;
N.K. Lowman, M.A. Hoefer, *Phys. Rev. A* 88 (2013) 013605.
- [17] J.E. Rothenberg, D. Grisckowsky, *Phys. Rev. Lett.* 62 (1989) 531;
J. Fatome, C. Finot, G. Millot, A. Armaroli, S. Trillo, *Phys. Rev. X* 4 (2014) 021022.
- [18] W. Wan, S. Jia, J.W. Fleischer, *Nat. Phys.* 3 (2007) 46;
N. Ghofraniha, C. Conti, G. Ruocco, S. Trillo, *Phys. Rev. Lett.* 99 (2007) 043903;
C. Conti, et al., *Phys. Rev. Lett.* 102 (2009) 083902;
W. Wan, S. Muenzel, J.W. Fleischer, *Phys. Rev. Lett.* 104 (2010) 073903;
N. Ghofraniha, et al., *Opt. Lett.* 37 (2012) 2325.
- [19] L. Bergé, et al., *Phys. Rev. Lett.* 89 (2002) 153902;
F. Bragheri, et al., *Phys. Rev. A* 76 (2007) 025801;
G.A. El, et al., *Phys. Rev. A* 76 (2007) 053813;
P. Whalen, et al., *Phys. Rev. A* 86 (2012) 033806;
M. Conforti, F. Baronio, S. Trillo, *Opt. Lett.* 37 (2012) 1082;
M. Crosta, A. Fratalocchi, S. Trillo, *New J. Phys.* 14 (2012) 093019;
S. Wabnitz, C. Finot, J. Fatome, G. Millot, *Phys. Lett. A* 377 (2013) 932–939;
M. Conforti, S. Trillo, *Opt. Lett.* 38 (2013) 3815;
M. Conforti, F. Baronio, S. Trillo, *Phys. Rev. A* 89 (2014) 013807;
A. Moro, S. Trillo, *Phys. Rev. E* 89 (2014) 023202;
M. Conforti, A. Mussot, A. Kudlinski, S. Trillo, *Sci. Rep.* 5 (2015) 9433.
- [20] E. Bettelheim, A.G. Abanov, P. Wiegmann, *Phys. Rev. Lett.* 97 (2006) 246401;
P. Wiegmann, *Phys. Rev. Lett.* 108 (2012) 206810.
- [21] P. Lorenzoni, S. Paleari, *Physica D* 221 (2006) 110;
A. Molinari, C. Daraio, *Phys. Rev. E* 80 (2009) 056602.
- [22] N.K. Lowman, M.A. Hoefer, *J. Fluid Mech.* 718 (2013) 524–557;
N.K. Lowman, M.A. Hoefer, *Phys. Rev. E* 88 (2013) 023016;
N.K. Lowman, M.A. Hoefer, G.A. El, *J. Fluid Mech.* 750 (2014) 372–384.
- [23] Y.C. Mo, et al., *Phys. Rev. Lett.* 110 (2013) 084802.
- [24] A. Fratalocchi, A. Armaroli, S. Trillo, *Phys. Rev. A* 83 (2011) 053846.
- [25] N. Ghofraniha, S. Gentilini, V. Follie, E. Del Re, C. Conti, *Phys. Rev. Lett.* 109 (2012) 243902;
S. Gentilini, N. Ghofraniha, E. Del Re, C. Conti, *Phys. Rev. A* 87 (2013) 053811.
- [26] J. Garnier, G. Xu, S. Trillo, A. Picozzi, *Phys. Rev. Lett.* 111 (2013) 113902.
- [27] G. Xu, D. Vocke, D. Faccio, J. Garnier, T. Roger, S. Trillo, A. Picozzi, *Nature Comm.* 6 (2015) 8131.
- [28] D.J. Benney, P.G. Saffman, *Proc. R. Soc. Lond. Ser. A Math. Phys. Eng. Sci.* 289 (1966) 301–320;
D.J. Benney, A.C. Newell, *Stud. Appl. Math.* 48 (1969) 29–53.
- [29] V.E. Zakharov, V.S. L'vov, G. Falkovich, *Kolmogorov Spectra of Turbulence I*, Springer, Berlin, 1992.
- [30] A.C. Newell, B. Rumpf, *Annu. Rev. Fluid Mech.* 43 (2011) 59–78.
- [31] A.C. Newell, S. Nazarenko, L. Biven, *Physica D* 152–153 (2001) 520–550.
- [32] V. Zakharov, F. Dias, A. Pushkarev, *Phys. Rep.* 398 (2004) 1–65.
- [33] S. Nazarenko, *Wave Turbulence*, in: *Lectures Notes in Physics*, Springer, 2011.
- [34] S.L. Musher, A.M. Rubenchik, V.E. Zakharov, *Phys. Rep.* 252 (1995) 177.
- [35] A. Picozzi, J. Garnier, T. Hansson, P. Suret, S. Randoux, G. Millot, D. Christodoulides, *Phys. Rep.* 542 (2014) 1–132.
- [36] J. Laurie, U. Bortolozzo, S. Nazarenko, S. Residori, *Phys. Rep.* 514 (2012) 121–175.
- [37] A.C. Newell, B. Rumpf, V.E. Zakharov, *Phys. Rev. Lett.* 108 (2012) 194502.
- [38] E. Turitsyna, G. Falkovich, V. Mezentsev, S. Turitsyn, *Phys. Rev. A* 80 (2009) 031804;
E. Turitsyna, et al., *Nature Photonics* 7 (2013) 783;
D.V. Churkin, et al., *Nature Comm.* 6 (2015) 6214. <http://dx.doi.org/10.1038/ncomms7214>;
S.K. Turitsyn, et al., *Nature Photon.* 9 (2015) 608.
- [39] A.C. White, B.P. Anderson, V.S. Bagnato, *PNAS* 111 (2014) 4719–4726.
- [40] M. Onorato, S. Residori, U. Bortolozzo, A. Montina, F.T. Arecchi, *Phys. Rep.* 528 (2013) 47–89.
- [41] M. Onorato, A. Osborne, R. Fedele, M. Serio, *Phys. Rev. E* 67 (2003) 046305.
- [42] S. Randoux, P. Walczak, M. Onorato, P. Suret, *Phys. Rev. Lett.* 113 (2014) 113902;
P. Walczak, S. Randoux, P. Suret, *Phys. Rev. Lett.* 114 (2015) 143903.
- [43] G. Xu, J. Garnier, S. Trillo, A. Picozzi, *Phys. Rev. A* 90 (2014) 013828.
- [44] A. Picozzi, S. Pitois, G. Millot, *Phys. Rev. Lett.* 101 (2008) 093901;
C. Michel, et al., *Phys. Rev. A* 83 (2011) 023806.
- [45] B. Kibler, et al., *Phys. Rev. E* 84 (2011) 066605;
G. Xu, et al., *Opt. Lett.* 38 (2013) 2972; *Opt. Lett.* 39 (2014) 4192.
- [46] J. Dudley, J.R. Taylor, *Supercontinuum Generation in Optical Fibers*, Cambridge University Press, Cambridge, 2010.
- [47] P. Constantin, P. Lax, A. Majda, *Comm. Pure Appl. Math.* 38 (1985) 715–724.
- [48] T. Benjamin, *J. Fluid Mech.* 29 (1967) 559;
H. Ono, *J. Phys. Soc. Japan* 39 (1975) 1082;
A. Fokas, M. Ablowitz, *Stud. Appl. Math.* 68 (1983) 1;
R. Coifman, V. Wickerhauser, *Inverse Problems* 5 (1990) 825;
S.Yn. Dobrokhotov, I.M. Krichever, *Math. Notes* 49 (1991) 583.
- [49] M.C. Jorge, A.A. Minzoni, N.F. Smyth, *Physica D* 132 (1999) 1;
P.D. Miller, Z. Xu, *Comm. Pure Appl. Math.* 64 (2011) 205; *Commun. Math. Sci.* 10 (2012) 117.
- [50] A. Picozzi, J. Garnier, *Phys. Rev. Lett.* 107 (2011) 233901.
- [51] V.E. Zakharov, S.L. Musher, A.M. Rubenchik, *Phys. Rep.* 129 (1985) 285–366.
- [52] M. Segev, D. Christodoulides, *Incoherent Solitons*, in: S. Trillo, W. Torruellas (Eds.), *Spatial Solitons*, Springer, Berlin, 2001.
- [53] Z. Chen, S.M. Sears, H. Martin, D.N. Christodoulides, M. Segev, *PNAS* 99 (2002) 5223.
- [54] T. Hansson, M. Lisak, D. Anderson, *Phys. Rev. Lett.* 108 (2012) 063901; *Phys. Rev. E* 84 (2011) 056601;
T. Hansson, D. Anderson, M. Lisak, V.E. Semenov, U. Osterberg, *J. Opt. Soc. Amer. B* 25 (2008) 1780.
- [55] A. Campa, T. Dauxois, S. Ruffo, *Phys. Rep.* 480 (2009) 57.
- [56] A. Campa, T. Dauxois, D. Fanelli, S. Ruffo, *Physics of Long-range Interacting Systems*, Oxford Univ. Press, 2014.
- [57] Y. Kivshar, G. Agrawal, *Optical Solitons: From Fibers to Photonic Crystals*, Academic Press, 2003.
- [58] G. Xu, J. Garnier, M. Conforti, A. Picozzi, *Opt. Lett.* 39 (2014) 4192.
- [59] C. Connaughton, et al., *Phys. Rev. Lett.* 95 (2005) 263901;
G. During, A. Picozzi, S. Rica, *Physica D* 238 (2009) 1524;
P. Aschieri, et al., *Phys. Rev. A* 83 (2011) 033838.
- [60] M. Peccianti, C. Conti, G. Assanto, A. De Luca, C. Umetsu, *Nature* 432 (2004) 733–737;
C. Conti, M. Peccianti, G. Assanto, *Phys. Rev. Lett.* 92 (2004) 113902.
- [61] C. Rotschild, B. Alfassi, O. Cohen, M. Segev, *Nat. Phys.* 2 (2006) 769;
C. Rotschild, O. Cohen, O. Manela, M. Segev, T. Carmon, *Phys. Rev. Lett.* 95 (2005) 213904.
- [62] C. Rotschild, T. Schwartz, O. Cohen, M. Segev, *Nature Photonics* 2 (2008) 371.
- [63] S. Turitsyn, *Theoret. Math. Phys.* 64 (1985) 226;
O. Bang, et al., *Phys. Rev. E* 66 (2002) 046619;
J. Wyllie, et al., *Phys. Rev. E* 66 (2002) 066615;
A. Dreischuh, et al., *Phys. Rev. Lett.* 96 (2006) 043901;
D. Buccoliero, A.S. Desyatnikov, W. Krolikowski, Y.S. Kivshar, *Phys. Rev. Lett.* 98 (2007) 053901;
B.K. Esbensen, A. Wlotzka, M. Bache, O. Bang, W. Krolikowski, *Phys. Rev. A* 84 (2011) 053854;
B.K. Esbensen, M. Bache, O. Bang, W. Krolikowski, *Phys. Rev. A* 86 (2012) 033838;
Q. Kong, et al., *Phys. Rev. A* 87 (2013) 063832.
- [64] W. Krolikowski, et al., *J. Opt. B: Quant. Semic. Opt.* 6 (2004) S288.
- [65] M.A. Baranov, *Phys. Rep.* 464 (2008) 71–111.
- [66] C. Jossierand, Y. Pomeau, S. Rica, *Phys. Rev. Lett.* 98 (2007) 195301.
- [67] S. Skupin, M. Saffman, W. Krolikowski, *Phys. Rev. Lett.* 98 (2007) 263902;
S. Sevincli, N. Henkel, C. Ates, T. Pohl, *Phys. Rev. Lett.* 107 (2011) 153001.
- [68] T.B. Gatski, J.P. Bonnet, *Compressibility, Turbulence and High Speed Flow*, Acad. Press, Elsevier, 2013.
- [69] A.C. Newell, P.J. Aucoin, J. Fluid Mech. 49 (1971) 593–609;
V.S. L'vov, Yu. L'vov, A.C. Newell, V. Zakharov, *Phys. Rev. E* 56 (1997) 390–405.
- [70] C. Michel, B. Kibler, J. Garnier, A. Picozzi, *Phys. Rev. A* 86 (2012) 041801(R);
B. Kibler, C. Michel, J. Garnier, A. Picozzi, *Opt. Lett.* 37 (2012) 2472;
G. Xu, J. Garnier, A. Picozzi, *Opt. Lett.* 39 (2014) 590–593.
- [71] J. Garnier, J.-P. Ayanides, O. Morice, *J. Opt. Soc. Amer. B* 20 (2003) 1409.
- [72] L.D. Landau, *J. Phys. USSR* 10 (1946) 25. (English translation in *J. Exp. Theor. Phys.* 16, 574).
- [73] D.N. Christodoulides, T.H. Coskun, M. Mitchell, Z. Chen, M. Segev, *Phys. Rev. Lett.* 80 (1998) 5113;
Z. Chen, M. Mitchell, M. Segev, T.H. Coskun, D.N. Christodoulides, *Science* 280 (1998) 889;
T.H. Coskun, D.N. Christodoulides, M. Mitchell, Z. Chen, M. Segev, *Opt. Lett.* 23 (1998) 418.
- [74] T.H. Coskun, D.N. Christodoulides, Z. Chen, M. Segev, *Phys. Rev. E* 59 (1999) R4777.
- [75] L.C. Evans, *Partial Differential Equations*, AMS, Providence, 2002.
- [76] See, e.g. C.D. Levermore, *J. Stat. Phys.* 83 (1996) 1021.
- [77] S.N. Gurbatov, A.I. Saichev, S.F. Shandarin, *Mon. Not. R. Astron. Soc.* 236 (1989) 385.
- [78] I. Bernstein, J. Green, M. Kruskal, *Phys. Rev.* 108 (1957) 546.
- [79] A. Hasegawa, *Phys. Fluids* 18 (1975) 77.
- [80] B. Eliasson, P.K. Shukla, *Phys. Rep.* 422 (2006) 225.